

Evaluation of High Frequency Electromagnetic Behavior of Planar Inductor Designs for Resonant Circuits in Switching Power Converters

A. Nejadpak, M. R. Barzegaran, and O. A. Mohammed

Energy Systems Research Laboratory, Department of Electrical and computer Engineering
Florida International University, Miami, FL, 33174, USA
mohammed@fiu.edu

Abstract — In this paper, a planar inductor based resonant circuit is designed for zero-current switching (ZCS) buck converter. In order to evaluate the actual behavior of the converter at the design stage, a numerical model of the inductor was created and implemented using the finite element (FE) analysis. Using the numerical model, a high frequency physics based circuit model was obtained for the converter's resonant circuit. The acquired physics based circuit model was used to approximate the electrical behavior of the resonant circuit. The operating condition of the half-wave ZCS buck converter was verified both numerically and experimentally. It was shown that by using the proposed high frequency model, it is possible to evaluate realistic waveforms of voltages and currents including the effects of parasitic elements. This is an essential step for studying conducted electromagnetic field emissions in power converters for the evaluation of their EMI interactions for EMC compliant designs.

Index Terms — EMI, EMC, finite element analysis, high frequency modeling, planar inductor, quasi-resonant converters.

I. INTRODUCTION

Soft-switching converters are becoming more popular as they have lower loss and noise characteristics as compared to pulse width modulation (PWM) converters. In these types of converters, the resonance circuit is a major contributor to the creation of EMI. It can cause unexpected current noise flow in the common mode path [1].

Generally, in order to control the conducted emissions (CE) noise in the soft-switching converters, the issue of parasitic elements must be considered during the design stage. These parasitics are circuit elements (resistance, inductance, or capacitance) that are possessed by electrical components, but are not desirable for them to have it.

So far, various algorithms were introduced to eliminate or minimize the effects of these unwanted elements [2-4]. Previously, methods based on the parallel-plate waveguide and FEM analysis was introduced to solve the PCB unwanted coupling problems and reduce the EMI effects of the converters [5-8].

All components and interconnections contain unintentional (parasitic) circuit elements which often a combination of them can make a change in the operating condition of the whole power converter. This makes the EMI issues more complicated. Furthermore, the switching action causes various parasitic elements in the converter and result in conducted and radiated energy at unpredictable frequencies. In practice, these parasitic oscillation frequencies are most difficult to filter out. They often cause the most interference with signal processing circuitry.

Therefore, an understanding of the magnitude of these parasitic elements and the characteristics of the components over a range of frequencies will ensure the correct choice of their application. Also, it is important for investigation of the effects of switching-frequency control on EMI generation.

The operating principle of the Quasi-resonant converters is described in [9]. These converters are

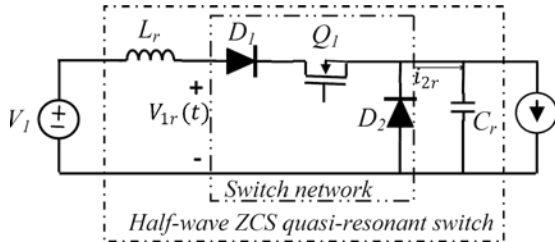


Fig. 1. Half wave zero current switching buck converter's circuit model.

obtained by adding the resonant elements L_r and C_r to the PWM switching converters. Figure 1 shows the simplified circuit model for ZCS-Buck converter. The parasitic elements in the configuration of the resonant components can affect the operating condition of the whole converter. In order to have a more precise study on the converter behavior, a distributed model should be obtained for each of the elements.

In this paper, a planar inductor based resonant circuit is designed for the converter's resonant inductor (shown by L_r in Fig. 1). This design can meet the packaging constraints in power electronic converters in addition to the required EMI compliance levels. Design and characteristic optimization of the planar inductor is studied in references [10-13]. The electromagnetic radiation of a PCB planar inductor is discussed in [14, 15]. As an example, based on the procedure in reference [9], the inductance value is selected to be $L_r = 1\mu\text{H}$, and the resonant capacitor is selected to be $C_r = 400\text{nf}$. With this selection, the resonant frequency will be $f_0 = \frac{1}{2\pi\sqrt{L_r C_r}} = 251.65\text{ kHz}$.

Subsequently, in order to find the parameters of the converter, a finite element analysis is performed on the resonant part of the converter. After obtaining the high frequency physics based model of the resonant circuit, the resonant behavior of the proposed planar inductor based resonant circuit is compared with the ideal resonant circuit. The FE analysis is used to study the electromagnetic behavior of the proposed resonant circuits in Section II of this paper. As a result, a high frequency model is obtained for the resonant circuit under a wide range of switching frequencies. Finally, the resonant circuit design was optimized in order to compensate the destructive effects of parasitic elements in the

operation of the converter. The results were verified through simulations and experimentation.

II. DISTRIBUTED-PARAMETER FREQUENCY DEPENDENT MODELING

Under PWM operating conditions, the inductor's resistance, inductance, and capacitance behave differently from the low frequency operation. The windings have skin and proximity effects, which cause the resistance to be much higher than the low frequency value. The inductance value decreases with the increase in the operating frequency, while the small capacitance effect comes in the picture at high frequencies. Under such PWM operation, the inductor winding's capacitance is distributed between several parts of the winding (turn to turn and turn to ground). Hence, to obtain accurate values of the resistances, inductances (self and mutual), and capacitances (self and mutual), a detailed numerical model for the inductor should be used. Also, this strategy is used for the capacitor of the converter since, in higher frequencies, the self and mutual inductances as well as the self and mutual capacitances have effects in the frequency response analysis.

In reference [16], a method based on the vector fitting algorithm was proposed for modeling the physics-based representation of transformers. This is also applicable to the inductor design. The method used in this study is based on the lumped-parameter model presented in [17, 18]. This method is used to obtain the s-domain model of a spiral winding planar inductor, which can be used to find the frequency response of the inductor. The proposed model includes the windings' resistances, self inductances, ground capacitances, the inter-turn capacitances within each winding and the mutual inductive and capacitive couplings between the two windings.

A. Physics based modeling using FEM

A three dimensional finite element study was performed on the resonant circuit components, in order to calculate the parasitic elements of these components, which can affect the operating condition of the converter.

The electromagnetic field inside the inductor and capacitor is governed by the following set of nonlinear partial differential equations [17]:

$$\vec{\nabla} \times \left((v) \vec{\nabla} \times \vec{A} \right) = \vec{J}, \quad (1)$$

$$\nabla \cdot \sigma \left(\frac{\partial \vec{A}}{\partial t} + \nabla V \right) = 0, \quad (2)$$

where \vec{A} is the magnetic vector potential, \vec{J} is the total current density, v is the magnetic reluctivity, V is the electric scalar potential, and σ is the electric conductivity. By solving these equations, the resistance and inductance of the inductor are calculated as a function of frequency.

Also, the electrostatic problem is solved for the calculation of capacitances matrix, as capacitances are a function of geometry rather than frequency. An electrostatic analysis is assumed to be a linear analysis, which means that the electric field is proportional to the applied voltage. The analysis determines the electric scalar potential distribution caused by the applied voltage. The following Maxwell equation is solved during electrostatic analysis.

$$\nabla \cdot (\epsilon \nabla V) = -\rho, \quad (3)$$

where ρ is surface charge density, ϵ is permittivity, V is electric scalar potential. By coupling electric and magnetic analyses, electromagnetic analysis for frequency response analysis based on (6) are applied in this simulation.

Typically, the quasi-static electromagnetic analysis is used as analysis approach in these cases, but this method has one problem. The changing electric displacement field over time is considered as zero ($\partial D / \partial t = 0$). This assumption can be used for low frequency analysis. However, for higher frequency analysis this assumption affects the result [19, 20]. Therefore, a new approach was used in this research in which $\partial D / \partial t$ is considered.

To derive the time harmonic equation, this physics interface solves magnetic and electric interface. The analysis is started with Maxwell-Ampere's law including the displacement current. This does not involve any extra computational cost in the frequency domain. Firstly, a time-harmonic field is assumed as (4).

$$\nabla \times \mathbf{H} = \mathbf{J} = \sigma(\mathbf{E} + v \times \mathbf{B}) + j\omega \mathbf{D} + \mathbf{J}^e. \quad (4)$$

Using the definitions of the fields $\mathbf{B} = \nabla \times \mathbf{A}$ and $\mathbf{E} = -\nabla V - j\omega \mathbf{A}$ and combine them with the constitutive relationships $\mathbf{B} = \mu_0(\mathbf{H} + \mathbf{M})$ and $\mathbf{D} = \epsilon_0 \mathbf{E}$, the Ampere's law can be rewritten as (5).

$$(j\omega\sigma - \omega^2\epsilon_0)\mathbf{A} + \nabla \times (\mu_0^{-1}\nabla \times \mathbf{A} - \mathbf{M}) - \sigma v \times (\nabla \times \mathbf{A}) + (\sigma + j\omega\epsilon_0)\nabla V = \mathbf{J}^e. \quad (5)$$

The equation of continuity is again obtained by taking the divergence of Ampere's law. It is the equation solved for the electric potential. Thus, the following equations for V and \mathbf{A} are achieved

$$-\nabla \cdot ((j\omega\sigma - \omega^2\epsilon_0)\mathbf{A} - \sigma v \times (\nabla \times \mathbf{A}) + (\sigma + j\omega\epsilon_0)\nabla V - (\mathbf{J}^e + j\omega\mathbf{P})) = 0. \quad (6)$$

A particular gauge can be obtained with reducing the system of equation by choosing $\Psi = -jV/\omega$ in the gauge transformation. So modified magnetic vector potential is obtained.

$$\tilde{\mathbf{A}} = \mathbf{A} - \frac{j}{\omega} \nabla V. \quad (7)$$

Working with $\tilde{\mathbf{A}}$ is often the best option when it is possible to specify all source currents as external currents \mathbf{J}^e or as surface currents on boundaries.

$$(j\omega\sigma - \omega^2\epsilon_0)\tilde{\mathbf{A}} + \nabla \times (\mu_0^{-1}\nabla \times \tilde{\mathbf{A}} - \mathbf{M}) - \sigma v \times (\nabla \times \tilde{\mathbf{A}}) + (\sigma + j\omega\epsilon_0)\nabla V = \mathbf{J}^e + j\omega\mathbf{P}, \quad (8)$$

where \mathbf{A} is magnetic potential, \mathbf{J}^e is external current density, \mathbf{M} is magnetization, and v is the motion speed which here, it is equal to zero.

The equation (8) is a modified version of a classic quasi-static equation (5), which is implemented in FE softwares [21]. Further modification in this study is applied by linking MATLAB software with FE software. This can be done by defining a variable in MATLAB codes as \mathbf{D} and making a link to the FE software, then considering this \mathbf{D} (electric displacement field) instead of the default \mathbf{D} . This new defined electric displacement field is based on the electric field obtained from the solution of software. The other element ($\tilde{\mathbf{A}}$) is defined in the same way.

Another necessity of this type of analysis is the need of simultaneous estimation of capacitance and inductance that the former one can be calculated by electrostatic analysis and the latter one by magnetostatic analysis. This type of interface can be used for 3D, 2D in-plane, and 2D axisymmetric models. Note that the magnetic and electric currents physics interface supports the stationary and frequency domain study types better than transient domain study.

Figure 2 shows the planar spiral inductor and capacitor models used in the power converter. To

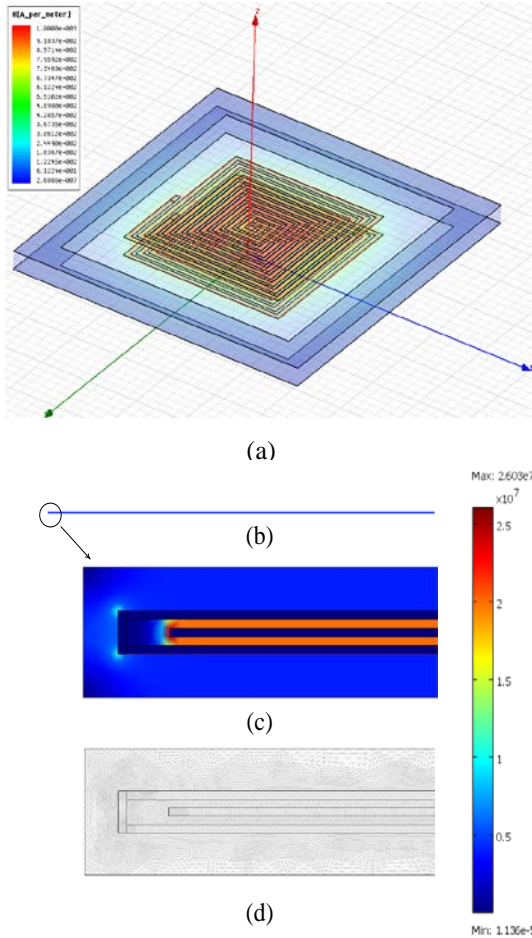


Fig. 2. Field spectrum from the finite element analysis for the calculation of high frequency model of this component. (a) Magnetic field intensity of spiral planar inductor, (b) capacitor, (c) electric field in small part of the capacitor, (d) mesh in capacitor.

find a numerical solution for this problem, coupling of the FE and a circuit based analysis is utilized. The amount of energy, magnetic and electric field are estimated from the FE model. The results are then imported to the circuit-based software (Spice), in order to evaluate the performance of the whole circuit.

After solving the FE model, the inductance, capacitance, and resistive matrices were obtained via calculation of the energy matrix in the FE model. The magnetic energy is calculated by:

$$W = \frac{1}{2} \iiint_V \mu \cdot \text{Re}(\mathbf{H}_1 \cdot \mathbf{H}_1^*) dv + \frac{1}{2} \iiint_V \mu \cdot \text{Re}(\mathbf{H}_2 \cdot \mathbf{H}_2^*) dv + \frac{1}{2} \iiint_V \mu \cdot \text{Re}(\mathbf{H}_1 \cdot \mathbf{H}_2^*) dv, \quad (9)$$

where $\mathbf{H}_i, i = 1,2$ is the magnetic field intensity

inside the model and μ is the permeability of the model.

Following the calculation of the magnetic energy in the FE model, equation (9), all self and mutual inductances were estimated based on the magnetic energy value, [22, 2]. Also explanation about deriving capacitances and resistances is mentioned in the same references.

B. Numerical discussion

As it was discussed, a numerical technique based on the adaptive MEI-FEM (magnetic-electric interface finite element method) is used. This method has much more accurate result as compared to quasi-static electromagnetic finite element method, electrostatic finite element method, and magnetostatic finite element method. All experiments are performed on a x5677 dual core 3.47 GHz CPU and 192GB RAM. The iteration process is terminated when the normalized backward error (tolerance) is reduced by 10^{-3} .

To implement the MEI-FEM, the adaptive grouping method is used to reduce the memory consumption and captures the fine details of the structure. The simulation time for the analysis of the inductor with five million degrees of freedom and 10^{-3} percent tolerance of energy was 3 hours. Also, simulation time for the analysis of the capacitor with three million degrees of freedom, Fig. 2(d), with $1e^{-7}$ percent tolerance of energy was about 2 hours. Figure 3 shows the energy tolerance versus the number of degrees of freedom.

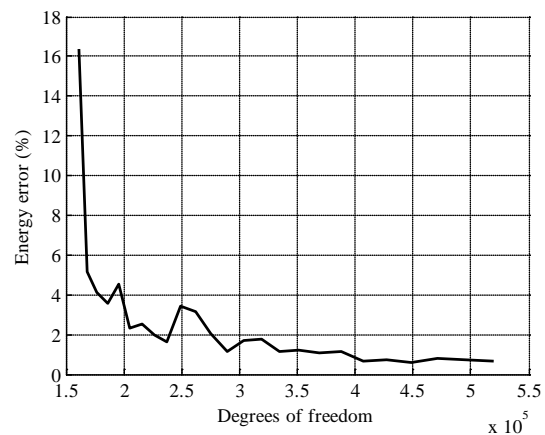


Fig. 3. Energy tolerance versus degrees of freedom.

The analysis method which is used in this analysis is the generalized minimal residual method (usually abbreviated GMRES) with successive over-relaxation (SOR) as pre and post smothers. GMRES is an iterative method for the numerical solution of a system of linear equations [23]. In numerical linear algebra, the method of SOR is a variant of the Gauss–Seidel method for solving a linear system of equations, resulting in faster convergence. A similar method can be used for any slowly converging iterative process. The SOR method uses a more accurate approximation of the matrix, which leads to fewer iterations but slightly more work per iteration than in the Jacobi method.

Since the geometry of the elements are non-uniform (the length of some elements are much bigger than the width of them). Geometric multi-grid method is chosen as the pre-conditioner and F-cycle as multi-grid cycle. Also, the parallel sparse direct linear solver (PARDISO) method with $1e^{-8}$ pivoting perturbation is chosen as the coarse solver.

C. Development of lumped-parameter model

The influence of the capacitive reactance is increased by increasing the switching frequency. Therefore, very small capacitive reactances can affect the input transfer function in higher frequencies. Besides, mutual inductances between elements at far distances are more significant in the transfer function in high frequencies. So, a model which considers all these reactances is essential. The distributed-section model considers almost all tiny capacitive reactances and mutual inductances, so it is eligible for high frequency analysis.

Following the calculation of all required parameters for the distributed model, these parameters are located in the model, then the model evaluation procedure starts. As in the lumped parameter model, the evaluation procedure from the distributed parameter nature of the problem at hand, we start at a location x and moving an infinitesimal distance Δx toward the lower end of the winding, the potential difference ΔV is calculated as:

$$\begin{bmatrix} \Delta V_1(x, s) \\ \Delta V_2(x, s) \end{bmatrix} = \begin{bmatrix} Z_1(s)\Delta x & Z_m(s)\Delta x \\ Z_m(s)\Delta x & Z_2(s)\Delta x \end{bmatrix} \begin{bmatrix} \hat{I}_1(x, s) \\ \hat{I}_2(x, s) \end{bmatrix}, \quad (10)$$

where $\hat{I}_1(x, s)$ and $\hat{I}_2(x, s)$ are the current following in Z_1 and Z_2 , respectively. The indices 1 and 2, indicates the first and the second layer of the inductor's and capacitor's models. A detailed description of this method is presented in reference [17]. By transferring the modal domain into a phase domain, the voltages of the top terminal in two layers are calculated as:

$$\begin{bmatrix} V_{s1}(s) \\ V_{s2}(s) \end{bmatrix} = \begin{bmatrix} M_{11}(s) & M_{12}(s) \\ M_{21}(s) & M_{22}(s) \end{bmatrix} \begin{bmatrix} I_{s1}(s) \\ I_{s2}(s) \end{bmatrix}, \quad (11)$$

where $M_{ij}(s)$ are elements of the impedance matrix in s-domain.

To determine the frequency characteristics of the inductor we set $s = j\omega$ in the related equations. The input impedance is given by:

$$Z_{in}(j\omega) = \frac{V_{s1}(j\omega)}{I_{s1}(j\omega)}. \quad (12)$$

Using the above equations, input impedance on the component is calculated as the following:

$$Z_{in}(j\omega) = M_{11}(j\omega). \quad (13)$$

The rational function given by (13) can be represented by an equivalent electrical network as shown in Fig. 4. Note that, the circuit model in Fig. 4 is not unique and can be shown in various configurations. This network reflects the frequency dependence of the inductor resistance, inductance and capacitance. Using $Z_{in}(j\omega)$, the natural frequencies are determined.

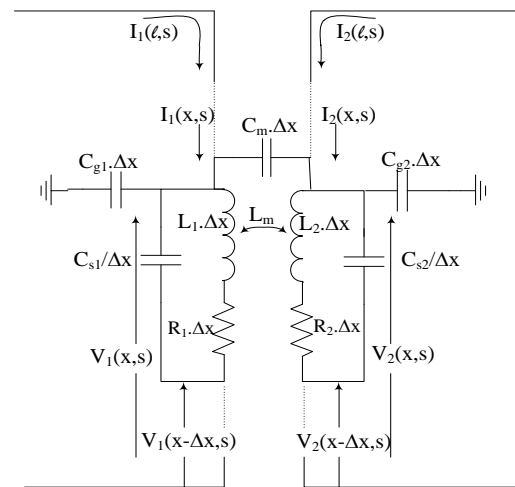


Fig. 4. Infinitesimal section of a two-layer winding of planar inductor.

The distributed model parameters of the designed inductor, from the finite element analysis were; $R_1=0.2713 \Omega$, $R_2=0.2713 \Omega$, $L_1=0.557 \mu\text{H}$, $L_2=0.557 \mu\text{H}$, $L_m=0.307 \mu\text{H}$, $C_{s1}=8 \text{ pF}$, $C_{s2}=8 \text{ pF}$, $C_{g1}=0.33 \text{ pF}$, $C_{g2}=0.33 \text{ pF}$, $C_m=6.7 \text{ pF}$. Also, the distributed model parameters of the capacitor were; $R_{c1,2,3}=0.006725 \Omega$, $R_{cm}=10 \text{ k}\Omega$, $L_{c1,2,3}=5 \text{ pH}$, $C_{s1,2,3}=0.49 \text{ pF}$, $C_{g1,2,3}=4.42 \text{ pF}$, $C_m=177 \text{ nF}$. As mentioned earlier, the indices 1 and 2 of the inductor parameters stand for the first and the second layers of the inductor, as shown in Fig. 2(b). Note that the neutral-end terminal point of the first layer is connected to the line-end terminal of the second layer.

An advantage of the distributed-parameter model is to reveal the high frequency behavior of the model. Therefore, using only simplified modeling of the resonant stage of HW ZCS-Buck converter doesn't show all the resonances and only shows the basic resonance as depicted in Fig. 5(a).

The embedded distributed model which is shown in Fig. 4 should have at least 5 sections to have reasonable result. We considered 10 sections in this study to have better and more accurate results. As mentioned in [17], the result will be more accurate with more number of sections but from specific number of section like 10 the results will not change significantly.

Utilizing the distributed parameter model developed in this paper, as shown in Fig. 5(b), a realistic picture emerges. The number of resonances becomes more practical and representative of the real device than the one given in Fig. 5(a). Accounting for parasitic resonances in higher frequencies will enable a realistic inclusion of EMC issues in the design stage. Through the optimization procedure [24], the size and geometry of the spiral planar inductor is changed in a way to minimize the effects of the parasitic parameters on the operating condition of the converter. The proposed algorithm is summarized as follows:

- Step 1: Design the planar inductor in the FE software.
- Step 2: Calculate the magnetic and electric fields based on equations (4)-(8).
- Step 3: Calculate resistances, inductances and capacitances based on equation (9).
- Step 4: Substituting the obtained parameters into the circuit shown in Fig. 4.

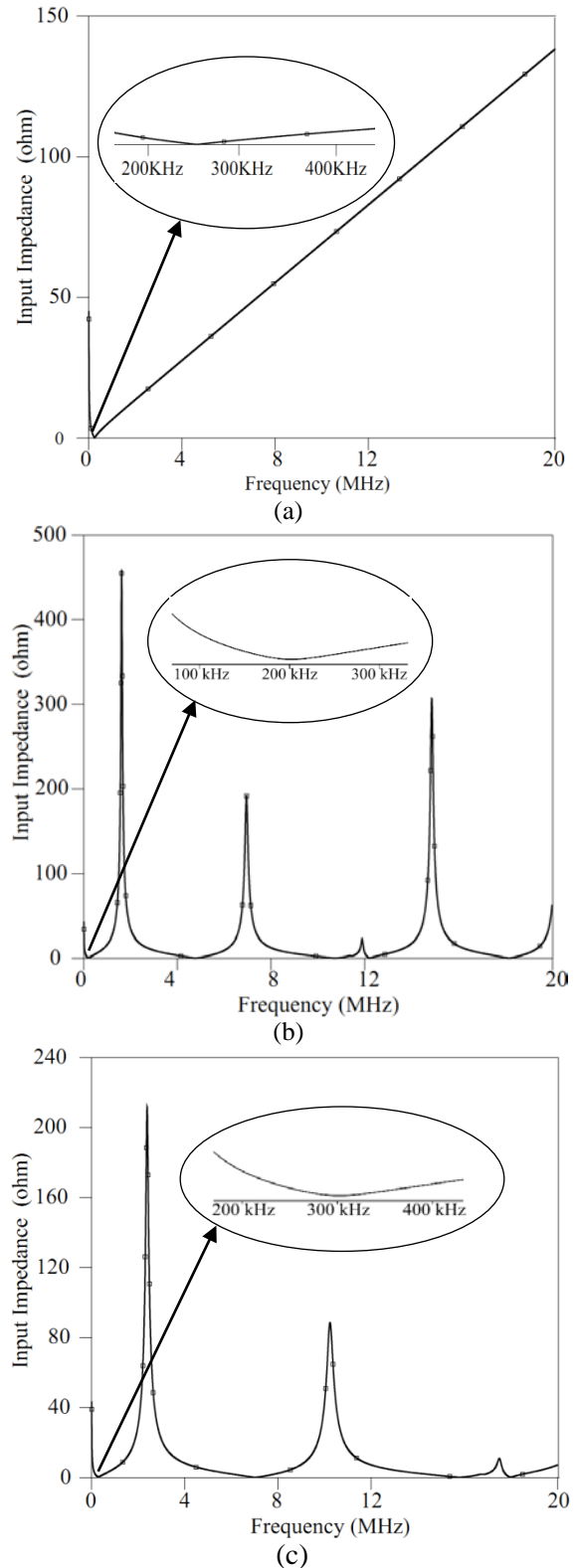


Fig. 5. Frequency response analysis of the ZCS buck converter. (a) Simple model, (b) distributed-parameter frequency model, (c) optimized distributed-parameter frequency model.

III. RESONANT CIRCUIT DESIGN OPTIMIZATION

As shown in Fig. 5, the first resonance frequency in Fig. 5(b) is much lower than the expected resonance frequency (the first resonance frequency shown in Fig. 5(a)). This phenomenon may deteriorate the operation of the converter. Because the resonance part of the converter is designed to resonate in 250 kHz (in this example) but in practice, it's resonating at lower frequencies.

In order to solve this problem, an optimization procedure is utilized in the design of the planar inductor. The main objective in the procedure of the optimization is to set the resonance frequency to the desired value (i.e 250 KHz), while reducing the amplitude of higher order harmonics. To achieve this goal, through the optimization process the planar inductor trace thickness and voltage clearance is changed as well as the number of turns. Therefore, a multi-objective function is formed as a combination of each of these single objectives. The first part of this multi-objective function is calculated from a transient non-linear FE analysis to calculate the value of the inductor. Moreover, the second part of this multi-objective function is calculated from the circuit simulation of the resonant circuit which is implemented in the Pspice environment. A classic genetic algorithm multi-objective optimization scheme is utilized to do the optimization task automatically. The variable of the genetic algorithm are indeed the inductance value of the planar inductor and magnitude of the harmonics in the resonant circuit output.

Figure 6 depicts the flowchart of the parameter optimizing procedure using GA. GA is a population based global search procedure which is inspired by natural selection and genetics law [25]. Parameters for optimization are number of turns in each layer (N) and inductor's trace dimensions. The GA evolves the given population of individuals. The objective function is as follows:

$$\text{Objective function} = \alpha_1 \cdot |\Delta f|^2 + \alpha_2 \cdot |Z_{in}(s)|^2$$

where, $\alpha_{1,2}$ =Weights signifying the importance of the objective function (taken as 1 in our case), Δf : frequency of the main resonance (resonant circuit first natural frequency) and $Z_{in}(s)$: input impedance of the resonant circuit. The main purpose of GA is to find the minimum for objective function.

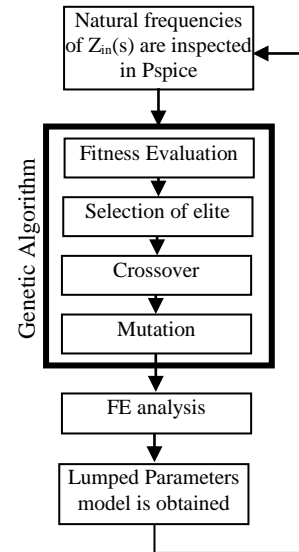


Fig. 6. The optimization process.

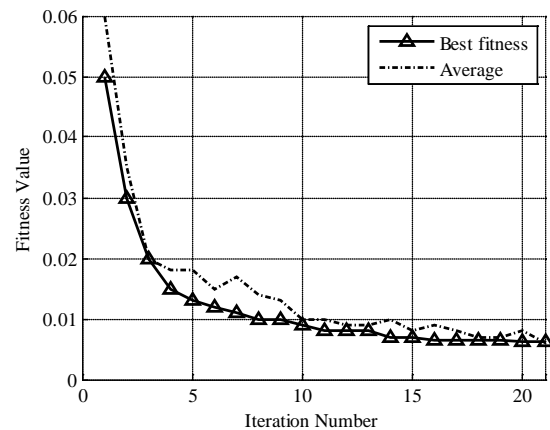


Fig. 7. Iteration accomplished by GA to minimize the objective function.

The fitness function computes the error of the simulated and specified reference signal at each time point. The errors are then squared and added together to give a single scalar objective value.

The fitness values shown in Fig. 7, illustrate that after about 10 number of iteration the error reaches to an acceptable value. Table 1 shows the results of the GA-algorithm and it is compared to the conventional inductors. Note that the optimization procedure is mainly applied on the design of the planar inductor and the resonance capacitor is not considered in the design optimization.

Table 1: Optimal values for designed inductor resulted from GA

Planar inductor design	L (μH)	Trace width (mil)	Number of turns
Un-optimized	1	40	8
Optimized	0.76	29.75	6

Figure 5(c) shows the frequency spectrum of the optimized resonant circuit. In Fig. 5(c), compared to Fig. 5(b), the unwanted higher frequency resonances are reduced. Also, the main resonance frequency is set to its desired value. (i.e. 250 KHz)

IV. RESULTS AND DISCUSSION

Figure 8 shows the experimental setup used to test and verify the results. In this setup, to inspect and record the results, a 600 MHz, 10 Gsample/s oscilloscope was used. The bandwidth for both the voltage and current probes were 100 MHz. The converter should operate in the zero-current switching condition. Therefore, the switching frequency and duty cycle is set by the digital function generator.

Figure 9 shows the effects of high-frequency operating conditions on the zero current switching (ZCS) of the MOSFET in the converter circuit. In this configuration, it was expected to increase the output voltage of the converter by increasing the operating frequency of the MOSFET, while keeping the ZCS sequence as shown in the ideal case (without considering all parasitic elements) shown in Fig. 9(a). The simulation results show that the ZCS behavior of the converter is completely lost as a result of using the high-frequency circuit model for the resonance circuit as shown in Fig. 9(b). The parameters in these circuits were evaluated from the FE implementation described in the previous section.

To keep the desired performance of the converter, the switching frequency of the converter should be kept below the value shown in Fig. 7(b). In an actual case (distributed-parameter frequency model), it can be observed from Fig. 7(b) that the next resonant frequencies, happen at the frequencies starting from 4.5 MHz and above. Figure 10 shows a comparison between two different designs of the resonant circuit. Figure 10(a) shows the FFT analysis of the primary design of the resonant circuit and Fig. 10(b) shows the FFT of the optimized resonant circuit output signal. It is noticed that, by design optimization the number and amplitude of

harmonics is reduced.

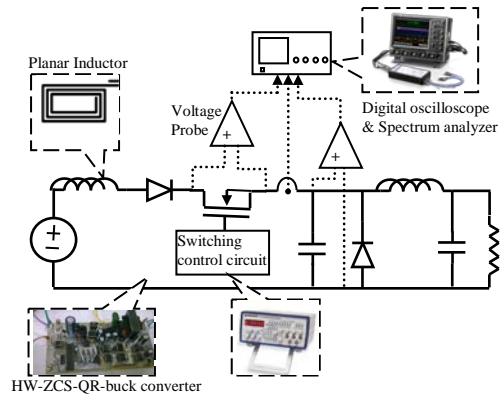
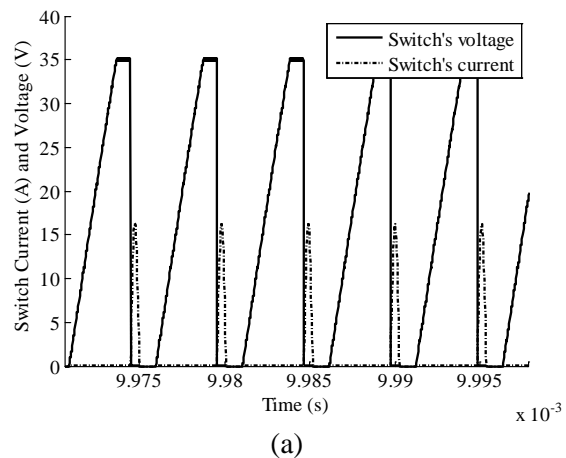


Fig. 8. Schematic of the converter’s experimental setup.

To verify the simulation results in Fig. 9, an experimental test was carried out. Figure 11 shows the measured voltage and current of the MOSFET, which is located in series with the resonance inductor (see Fig. 1). As it is illustrated in Fig. 11(a), in the primary design (un-optimized) of the resonance-circuit, by increasing, the switching frequency above a certain value the unwanted resonances will appear. These resonances can harm the proper zero-current switching operation of the converter.

Figure 11(b) shows the switch’s voltage and current, in the circuit with the optimized resonance circuit. As it is illustrated in this figure, the converter is operating in zero-current switching condition as it was expected.

In Fig. 11(a), some distortions are observed in the switch’s voltage waveform. These distortions are mainly because of the parasitic elements of the circuit and poor layout of the PCB, which are not considered in this study.



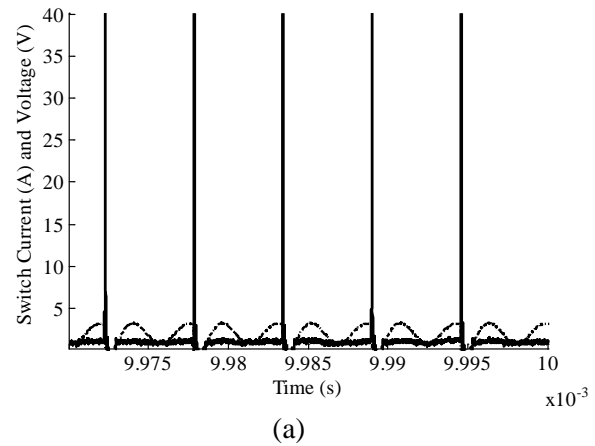
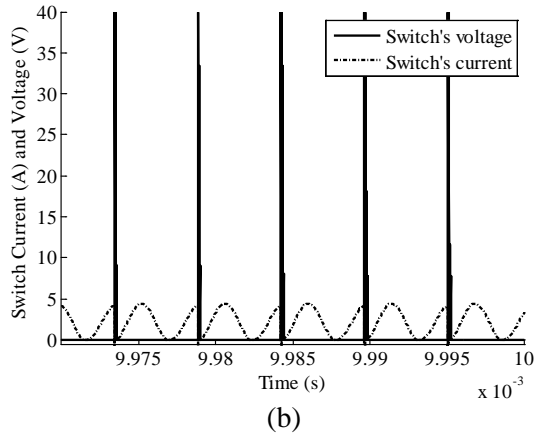


Fig. 9. Voltage and current of the switches in ZCS-Buck converter, (a) ideal case, (b) actual case.

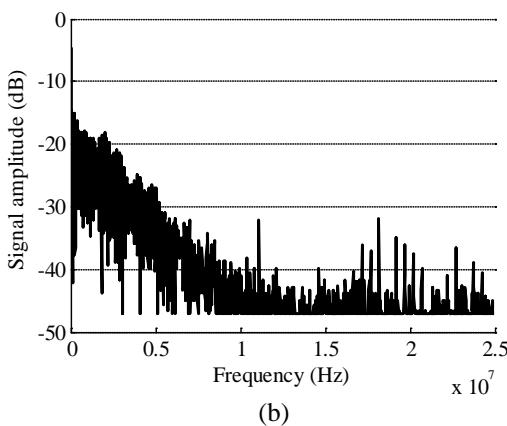
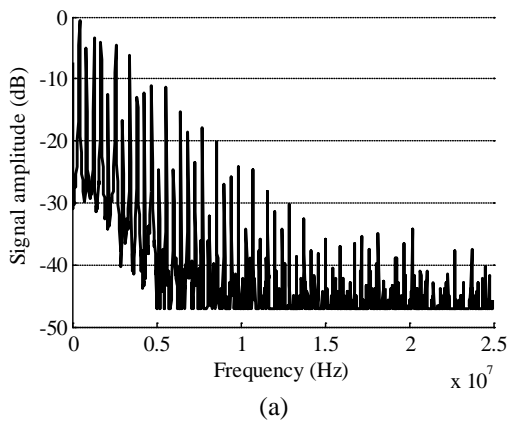


Fig. 10. FFT spectrum of the resonant circuit. a)Initial design, b) modified design.

V. CONCLUSIONS

In this paper, a method for high frequency model of the converter's components is presented using coupled circuit/electromagnetic FE computations. The FE analysis was performed to

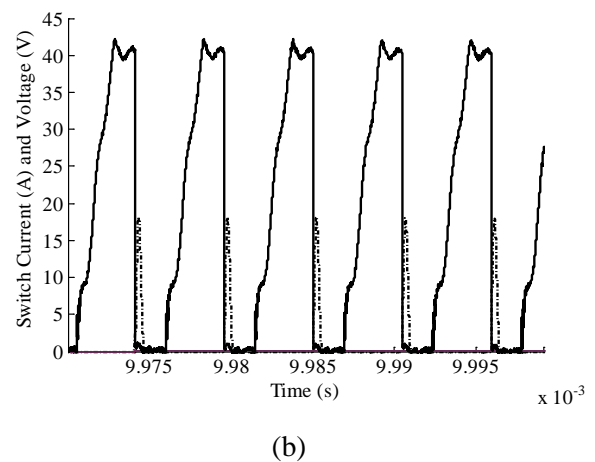


Fig. 11. Measured voltage and current of the switches in ZCS-Buck converter, (a) primary designed circuit, (b) optimized circuit.

obtain the frequency behavioral model of the converter. The natural frequencies computed from the proposed s-domain model, was used to analyze the circuit's electrical behavior and operation. The results show that the s-domain model of the converter has the ability to reveal the behavior of parasitic elements as well as higher resonances which has critical impact in studying EMI problems. This model can also be implemented for other types of converters making it practical for the evaluation on EMI/EMC issues in the design and development stages. The power converter discussed in this paper is not a representative of all power converter designs. But can show the value of considering the effects of parasitic components on operation of the power converters, especially when their switching frequencies are increased. By considering the effects of parasitic components,

one can modify the converter's circuit design in a way to reduce the effects of parasitic components and set the operating condition so that satisfies the converter's behavioral characteristics.

ACKNOWLEDGMENT

Part of this work was supported by a grant from the Office of Naval Research.

REFERENCES

- [1] M. Kchikach, R. Lee, H. F. Weinner, Y. Zidani, Y. S. Yuan, and Z. M. Qian, "Study of the Resonance Phenomenon in Switching Mode Power Supply (SMPS)," *Power Electronics Specialists Conference, 2004. PESC 04. 2004 IEEE 35th Annual*, vol. 4, pp. 3016- 3020, 2004.
- [2] S. V. Kulkarni, *Transformer Engineering: Design and Practice*, Marcel Dekker, Taylor & Francis Group, New York, May 2004.
- [3] S. Hashino and T. Shimizu, "Characterization of Parasitic Impedance in a Power Electronics Circuit Board using TDR," *Power Electronics Conference (IPEC), 2010 International*, pp. 900-905, June 21-24, 2010.
- [4] T.-H. Li, J. Wang, and H. S.-H. Chung, "Effect of Parasitic Elements in a Power Converter on the Switching Performance of a MOSFET-Snubber-Diode Configuration," *Applied Power Electronics Conference and Exposition (APEC), 2011 Twenty-Sixth Annual IEEE*, pp. 364-371, March 6-11, 2011.
- [5] M. R. Abdul-Gaffoor, H. K. Smith, A. A. Kishk, and A. W. Glisson, "Simple and Efficient Full-Wave Modeling of Electromagnetic Coupling in Realistic RF Multilayer PCB Layouts," *Microwave Theory and Techniques, IEEE Transactions on*, vol. 50, no. 6, pp. 1445-1457, Jun. 2002.
- [6] J.-G. Yook, L. P. B. Katehi, K. A. Sakallah, R. S. Martin, L. Huang, and T. A. Schreyer, "Application of System-Level EM Modeling to High-Speed Digital IC Packages and PCBs," *Microwave Theory and Techniques, IEEE Transactions on*, vol. 45, no. 10, pp. 1847-1856, Oct. 1997.
- [7] W. Chen, X. Yang, and Z. Wang, "Application of Wavelets and Auto-Correlation-Function for Cancellation of High-Frequency EMI Noise," *Applied Computational Electromagnetic Society (ACES) Journal*, vol. 24, no. 3, pp. 332 - 336, June 2009.
- [8] A. Bhargava, D. Pommerenke, K. W. Kam, F. Centola, and C. Lam, "DC-DC Buck Converter EMI Reduction Using PCB Layout Modification," *Electromagnetic Compatibility, IEEE Transactions on*, vol. 53, no. 3, pp. 806-813, Aug. 2011
- [9] R. W. Erickson and D. Maksimovic, *Fundamentals of Power Electronics*, Springer, p. 912, 2nd ed., 2001.
- [10] J. Yunas, N. A. Rahman, L. T. Chai, and B. Y. Majlis, "Study of Coreless Planar Inductor at High Operating Frequency," *Semiconductor Electronics, 2004. ICSE 2004. IEEE International Conference on*, p. 5, Dec. 7-9, 2004.
- [11] J. Vanek, I. Szendiuch, and J. Hladik, "Optimization of Properties of Planar Spiral Inductors," *Electronics Technology, 30th International Spring Seminar on*, pp. 235-238, May 9-13, 2007.
- [12] J.-J. Lee, Y.-K. Hong, S. Bae, J.-H. Park, J. Jalli, G. S. Abo, R. Syslo, B.-C. Choi, and G. W. Donohoe, "High-Quality Factor Ni-Zn Ferrite Planar Inductor," *Magnetics, IEEE Transactions on*, vol. 46, no. 6, pp. 2417-2420, June 2010.
- [13] A. Eroglu, "Microstrip Inductor Design and Implementation," *Applied Computational Electromagnetic Society (ACES) Journal*, vol. 25, no. 9, pp. 794 - 800, September 2010.
- [14] D. Hui, Z. Yisheng, and Z. Baishan, "Research on the Electromagnetic Radiation of a PCB Planar Inductor," *Microwave Conference Proceedings, 2005. APMC 2005. Asia-Pacific Conference Proceedings*, vol. 1, pp. 3, Dec. 4-7, 2005.
- [15] Z. Jonsener, "A New Calculation for Designing Multilayer Planar Spiral Inductors," *Electronics Design Strategy, News*. EDN, July 29, 2010.
- [16] N. Y. Abed and O. A. Mohammed, "Frequency Dependent Coupled Field-Circuit Modeling of Armored Power Cables using Finite Elements," *Electromagnetic Field Computation (CEFC), 2010 14th*

- Biennial IEEE Conference on*, pp.1-1, May 9-12, 2010.
- [17] A. S. Alfuhaid, "Frequency Characteristics of Single-Phase Two-Winding Transformers using Distributed-Parameter Modeling," *Power Delivery, IEEE Transactions on*, vol. 16, no. 4, pp. 637-642, Oct. 2001.
- [18] L. Satish and S. K. Sahoo, "An Effort to Understand What Factors Affect the Transfer Function of a Two-Winding Transformer," *Power Delivery, IEEE Transactions on*, vol. 20, no. 2, pp. 1430-1440, April 2005.
- [19] N. N. Rao, *Elements of Engineering Electromagnetics*, Prentice Hall, 6th Edition, pp. 321-324, 2004.
- [20] F. T. Ulaby, *Fundamental of Applied Electromagnetics*, Prentice Hall, 5th Edition, pp. 321-324, 2006.
- [21] M. R. Barzegaran, A. Nejadpak, and O. A. Mohammed, "High Frequency Electromagnetic Field Model for the Evaluation of Parasitic Elements in Power Converters," *27th Annual Review of Progress in Applied Computational Electromagnetics*, ACES March 27-31, pp. 623-629, 2011.
- [22] C. R. Paul, "INDUCTANCE Loop and Partial," published by John Wiley and Sons, 2010.
- [23] Y. Saad, *Iterative Methods for Sparse Linear Systems*, 2nd edition, Society for Industrial and Applied Mathematics, 2003.
- [24] A. Nejadpak, M. R. Barzegaran, A. Sarikhani, and O. A. Mohammed, "Design of Planar Inductor Based Z-Source Inverter for Residential Alternate Energy Sources," *Applied Power Electronics Conference and Exposition (APEC)*, 2011 Twenty-Sixth Annual IEEE, pp. 1698-1703, March 6-11, 2011.
- [25] D. E. Goldberg, *Genetic Algorithms in Search, Optimization and Machine Learning*, Addison-Wesley Longman Publishing Co., Inc. Boston, MA, USA, 1989.



Arash Nejadpak (S'09) received his B.S. in Electrical Engineering in 2007 and his M.S. degree in Power Electronics and Electric Machines from Sharif University of Technology, Tehran, Iran in 2009. Currently, he has been a graduate research assistant working towards his Ph.D. degree in Electrical Engineering at Florida International University, Miami, Florida since January 2010. His current research interests include intelligent control of PM machines and development of physics based models and design optimization of power electronic conversion systems.



Mohammadreza Barzegaran (S'10) Obtained B.Sc. and M.Sc. Degrees in Power Engineering from University of Mazandaran (Babol Institute of Technology), Iran in 2007 and 2010, respectively. He is currently pursuing the Ph.D. degree in the department of electrical and computer engineering, Florida International University, Florida, USA. His research interests include studying electromagnetic compatibility in power components, life assessment of electrical power components, fault detection in electrical machines, and also computer-aid simulation of power components.



Osama A. Mohammed (S'79, M'83, SM'84, F'94): Professor Mohammed received his M.S. and Ph.D. degrees in Electrical Engineering from Virginia Polytechnic Institute and State University. He has many years of teaching, curriculum development, research and industrial consulting experience. He authored and co-authored more than 300 technical papers in the archival literature as well as in National and International Conference records in addition to additional numerous technical and project reports and monographs. Professor Mohammed specializes in Electrical Energy Systems especially in areas related to alternate and renewable energy systems. He is also interested in design optimization of electromagnetic devices, Artificial Intelligence

Applications to Energy Systems as well as Electromagnetic Field Computations in Nonlinear Systems for these energy applications. He has current interest in Shipboard power systems and integrated motor drives. He is also interested in the application communication and sensor networks for the distributed control of power grids. Dr. Mohammed has been successful in obtaining a number of research contracts and grants from industries and Federal government agencies. He has a current active and funded research programs in several areas funded by the office of Naval Research and the US Department of Energy. Professor Mohammed is also interested in developing learning environments and educational techniques for Internet based delivery systems and virtual laboratories.

Professor Mohammed is a Fellow of IEEE and is a recipient of the 2010 IEEE PES Cyril Veinott Electromechanical Energy Conversion Award. Professor Mohammed is also a Fellow of the Applied Computational Electromagnetic Society. He is Editor of IEEE Transactions on Energy Conversion, IEEE Transactions on Magnetics-Conferences, as well as an Editor of COMPEL. He also received many awards for excellence in research, teaching and service to the profession and has chaired sessions and programs in

numerous International Conferences in addition to delivering numerous invited lectures at scientific organizations in around the world.

Professor Mohammed serves as the International Steering Committee Chair for the IEEE International Electric Machines and Drives Conference (IEMDC) and the IEEE Biannual Conference on Electromagnetic Field Computation (CEFC). Professor Mohammed was the General Chair of the 2009 IEEE IEMDC conference held in Miami Florida, May 3-6 2009 and was the Editorial Board Chairman for the IEEE CEFC2010 held in Chicago, IL USA, May 9-12, 2010. He was also the General Chairman of the 1996 IEEE International Conference on Intelligent Systems Applications to Power Systems (ISAP'96). Dr. Mohammed has chaired the Electric Machinery Committee for IEEE PES was the Vice Chair and Technical Committee Program Chair for the IEEE PES Electric Machinery Committee for a number of years. He was a member of the IEEE/Power Engineering Society Governing Board (1992-1996) and was the Chairman of the IEEE Power Engineering Society Constitution and Bylaws committee. He also serves as chairman, officer or as an active member on several IEEE PES committees, sub-committees and technical working groups.